arXiv:1509.08296v2 [cond-mat.mes-hall] 26 Jun 2016

Grand canonical Peierls transition in In/Si(111)

Eric Jeckelmann,[1,*] Simone Sanna,[2] Wolf Gero Schmidt,[2] Eugen Speiser,[3] and Norbert Esser[3]

[1] *Institut für Theoretische Physik, Leibniz Universität Hannover, Appelstr. 2, 30167 Hannover, Germany*
[2] *Lehrstuhl für Theoretische Materialphysik, Universität Paderborn, D-33095 Paderborn, Germany*
[3] *Leibniz-Institut für Analytische Wissenschaften, ISAS e.V., Schwarzschildstrasse 8, D-12489 Berlin, Germany*

(Dated: August 9, 2016)

Starting from a Su-Schrieffer-Heeger-like model inferred from first-principles simulations, we show that the metal-insulator transition in In/Si(111) is a first-order grand canonical Peierls transition in which the substrate acts as an electron reservoir for the wires. This model explains naturally the existence of a metastable metallic phase over a wide temperature range below the critical temperature and the sensitivity of the transition to doping. Raman scattering experiments corroborate the softening of the two Peierls deformation modes close to the transition.

PACS numbers: 71.10.Pm, 68.35.Rh, 68.43.Bc

A Peierls-like transition in indium wires on the Si(111) surface was first reported 16 years ago [1]. Since then this transition has been studied extensively [2–21] both experimentally and theoretically. The occurrence of both a metal-insulator transition around $T_c = 130K$ and a structural transition of the In wires from a 4×1 structure at room temperature to a 8×2 structure at low temperature are well established. Yet, the nature of the transition is still poorly understood and the relevance of the Peierls theory remains controversial [8, 9, 11, 12, 14, 19, 22].

The generic theory of Peierls systems is essentially based on effective models for the low-energy degrees of freedom in purely one-dimensional (1D) or strongly anisotropic three-dimensional (3D) crystals, such as the Ginzburg-Landau theory of 1D charge-density waves (CDW) [23] or the Su-Schrieffer-Heeger (SSH) model for conjugated polymers [24–28]. Hitherto it has been used without adaptation to discuss the relevance of the Peierls physics for experiments and first-principles simulations in In/Si(111). Thus a fundamental issue with previous interpretations based on these generic theories is that they do not consider how the 3D substrate affects the Peierls physics in a 1D atomic wire.

In this Rapid Communication, we investigate the phase transition in In/Si(111) theoretically using first-principles simulations and 1D model calculations, and experimentally with Raman spectroscopy. We show that it can be interpreted as a grand canonical Peierls transition, in which the substrate acts as a charge reservoir for the wire subsystem. The two Peierls distortion modes are essentially made of shear and rotary modes. The main difference with the usual (i.e., canonical) Peierls theory is that in the grand canonical theory the high-temperature phase can remain thermodynamically metastable below the critical temperature T_c and that the phase transition can become first order. This agrees with the interpretation of recent experiments and first-principles simulations in In/Si(111) [16–18, 20, 21].

First, we construct an effective 1D model for In/Si(111) in the spirit of the SSH model [24–27]. Our goal is a qualitative description of the phenomena with reasonable order of magnitudes for physical quantities because we think that a quantitative description of this complex material can only be achieved with first-principles simulations [29]. For the same reason, we neglect correlation effects [27, 28, 30, 31]. The accepted structural model for the uniform phase (i.e., the 4×1 phase) consists in parallel pairs of zigzag indium chains [32, 33]. We consider a single wire made of four parallel chains of indium atoms arranged on a triangular lattice as shown in Fig. 1. One (Wannier) orbital per indium atom is taken into account yielding four bands in the uniform phase. Density-functional theory (DFT) calculations actually show four bands corresponding to indium-related surface states [34]. Other electronic degrees of freedom, e.g. in the substrate, are not considered explicitly.

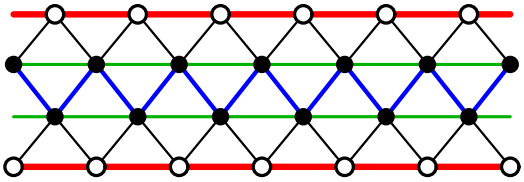

FIG. 1. (Color online) 1D lattice model for an indium wire in the uniform configuration. Open and full circles represent outer and inner In atoms, respectively. The line widths are proportional to the hopping terms t_{ij}. The blue and red bonds define the central zigzag chain and the two outer linear chains, respectively.

We use a tight-binding Hamiltonian model for the electronic degrees of freedom and assume that the only relevant hopping terms are between nearest-neighbor sites, i.e.,

$$H = \sum_{i,\sigma} \epsilon_i c^\dagger_{i\sigma} c_{i\sigma} - \sum_{\langle i,j\rangle,\sigma} t_{ij} \left(c^\dagger_{i\sigma} c_{j\sigma} + c^\dagger_{j\sigma} c_{i\sigma} \right) \qquad (1)$$

where the indices i, j number the indium atoms, $\sigma = \uparrow, \downarrow$ designs the electron spin, the second sum runs over every pair $\langle i, j\rangle$ of nearest-neighbor sites, and the operator $c^\dagger_{i\sigma}$ ($c_{i\sigma}$) creates (annihilates) an electron with spin

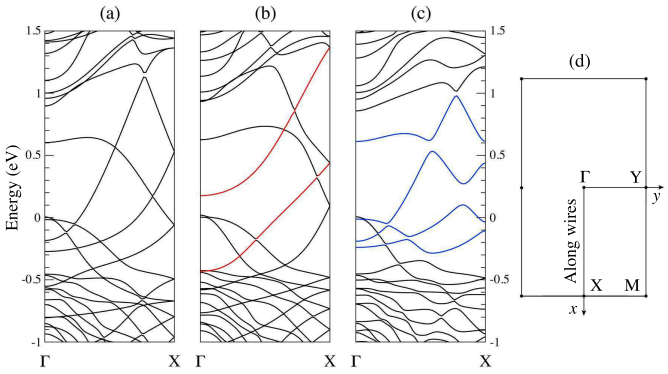

FIG. 2. (Color online) DFT-LDA electronic band structure of In/Si(111) (a) in the 4×1 phase, (b) after a shear distortion, and (c) after a rotary distortion in the surface Brillouin zone of the 4×2 configuration shown in (d). Gaps open (b) at Γ between two red bands and (c) close to X between four blue bands.

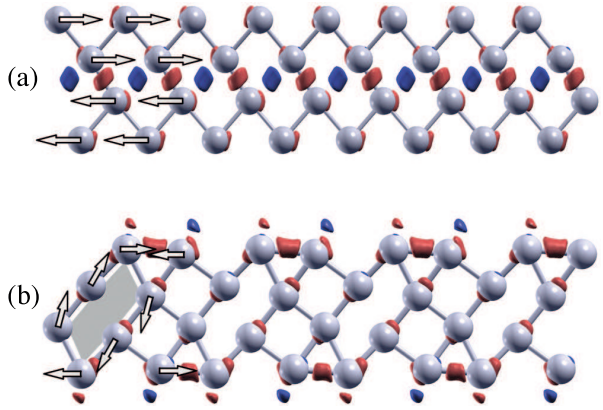

FIG. 3. (Color online) Changes in the DFT-LDA electronic densities (red for an increase, blue for a reduction) with respect to the 4×1 phase caused by (a) a shear distortion and (b) a rotary distortion. The isosurfaces for density changes ± 0.02 eÅ^{-3} are shown. Arrows show the atom displacements for both distortion modes

σ on site j. In the uniform phase the Hamiltonian is translationally invariant and the single-electron dispersions can be calculated analytically [29]. Thus we can determine parameters ϵ_i and t_{ij} to mimic the DFT band structure [17, 34] shown in Fig. 2(a). We obtain three metallic bands and one full band if we assume that the 1D system is close to half filling (i.e., one electron per orbital on average).

The strength of the hopping terms t_{ij} is shown in Fig. 1. Clearly, the apparent structures are a central zigzag chain and two outer linear chains. The bond order (electronic density in the bonds between atoms) exhibits a similar structure [29]. This is quite different from the usual representation of the 4×1 configuration by two zigzag chains. Our effective 1D model focuses on the metallic bands and thus reveals the bonds responsible for the Peierls instability.

In the hexamer structural model for the low-temperature phase, the deformation from the uniform to the dimerized (i.e., 8×2 or 4×2) phase corresponds essentially to the superposition of two rotary and one shear modes [8, 9, 11, 15, 17]. Therefore, we investigate the changes in the lattice structure, electronic band structure, and electronic density caused by each mode separately using first-principles frozen-phonon and deformation-potential calculations based on DFT within the local density approximation (LDA). The technical details correspond to earlier calculations by some of the present authors [14, 17]. A very recent hybrid DFT calculation [22] largely agrees with the DFT-LDA results presented here. We use distortion amplitudes close to the ones necessary to transform the zigzag structure into the hexagon structure. The predicted vibration modes agree well with Raman spectroscopy measurements presented here and in previous works [4, 12, 15].

This study reveals on the one hand that the main effects of the shear distortion are to dimerize the central zigzag chain, as shown by the alternating density and bond lengths between inner In atoms in Fig. 3(a), and to open or enlarge a gap between two metallic bands close to the Γ point as seen in Fig. 2(b). On the other hand, the main effects of the rotary modes are to dimerize the outer chains, as shown by the alternating density and bond lengths between outer atoms in Fig. 3(b), and to open a gap between two metallic bands close to the X point, as seen in Fig. 2(c). These results confirm the central role of the structures seen in Fig. 1 (i.e., one inner zigzag chain and two outer linear chains) in the transition of In/Si(111). Moreover, the negligible length and density variation for the bonds between inner and outer indium atoms in first-principles calculations, both for shear and rotation distortions, confirm that they are very strong covalent bonds and do not play any direct role in the transition.

The SSH model [24–27] is the standard model for the CDW on bonds caused by a Peierls distortion seen in Fig. 3. The bond length changes determined with first-principles methods can also be used to determine the hopping terms of the 1D model (1) for distorted lattice configurations. For this purpose, we assume that the hopping term between two orbitals i and j depends only on the distance d_{ij} between both atoms and choose the exponential form [35, 36]

$$t_{ij}\left(d_{ij}\right) = t_{ij} \exp\left[-\alpha_{ij}\left(d_{ij} - d_{ij}^{0}\right)\right] \qquad (2)$$

where t_{ij} and d_{ij}^{0} are the hopping terms and bond lengths in the uniform configuration. Using reasonable values for the electron-lattice couplings $t_{ij}\alpha_{ij}$ (i.e., α_{ij}^{-1} is of the order of the covalent radius of an In atom), we find a qualitative agreement between first-principles and 1D model predictions for the changes in the band structure and density caused by shear and rotary modes [29].

The mechanism of the Peierls transition can be understood even better by focusing on the main features of

the 1D model. Keeping only the most important hopping terms (thick lines in Fig. 1) and couplings to lattice distortions, the 1D model decouples into three independent chains with SSH-type Hamiltonians [24–27] and electron-lattice couplings (2): the inner zigzag chain which couples only to the shear mode and two identical outer linear chains which couple only to one of the two rotary modes each. To complete the SSH-type Hamiltonians we add an elastic potential energy for the lattice deformation. The free energy of each chain ($l = 1, 2, 3$) is then given by

$$F_l(x_l) = F_l^e(x_l) + \frac{K_l}{2} x_l^2 \tag{3}$$

where F_l^e is the electronic free energy [23]. Within this mean-field and semi-classical approach, the stable configurations are given by the minima of the total free energy $F = \sum_l F_l$ of the 1D model with respect to the amplitudes x_l of the three independent distortion modes. The bare elastic constants K_l can be estimated using the distortion amplitudes x_l necessary to form the hexamer structure in first-principles calculations [29].

This generalization of the SSH model includes more degrees of freedom than the generalized SSH model used very recently to investigate chiral solitons in indium wires [37]. Yet the model of Ref. [37] corresponds essentially to the restriction of our model to outer chains and rotary distortions. Furthermore, the model parameters found in Ref. [37] also agree quantitatively with our parameters for outer chains and rotary distortions [29]. In Ref. [22] Kim and Cho compare their DFT results to the two-chain SSH model of Ref. [37] and conclude that the transition in In/Si(111) is not a Peierls transition. However, their DFT results seem to agree largely with our three-chain SSH model and thus support the Peierls transition scenario presented here.

We can now analyze the 1D model in the mean-field approximation using known results for one-band/one-mode SSH-type models [24–27]. At half filling the outer chains have Fermi wave number $k_F = \pi/2$ and thus are unstable with respect to rotary distortions with the nesting wave number $Q = 2k_F = \pi$ [corresponding to the X point of the Brillouin zone in the 4×1 configuration of In/Si(111)]. As the zigzag chain has two orbitals per unit cell, its Fermi wave number is $k_F = \pi$ and thus it is unstable against a shear distortion with the nesting wave number $Q = 2k_F = 2\pi$ (corresponding to the Γ point). Therefore, if the system is exactly half filled, the twofold degenerate ground state of each chain is a band insulator with a dimerized lattice structure. The corresponding theoretical collective vibrational modes agree with the Raman spectroscopy results presented below.

This corresponds to an eightfold degenerate and insulating phase in the full 1D model. The neglected couplings between the three chains reduce the Peierls deformation modes to two linear combinations of the shear and rotary modes and the degeneracy to four states corresponding to the four hexamer structures of the 4×2 phase. The Peierls gap in the electronic band of the inner chain is at $k = 0$ while Peierls gaps for the outer chains are at $k = \pi/2$ (i.e., the X-point of the 4×2 configuration). Typically, the electronic gap of the full 1D model is indirect and smaller than the Peierls gaps. Thus there is no obvious relation between critical temperature and electronic gap in this many-band Peierls system. The structural transition to the high-temperature uniform phase is continuous but may exhibit distinct critical temperatures for shear and rotary modes. The metal-insulator transition occurs at the lowest one.

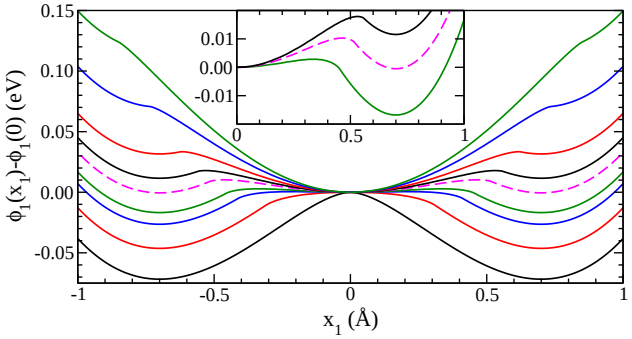

FIG. 4. (Color online) Grand canonical potential ϕ_1 of the inner zigzag chain as a function of the amplitude of the shear distortion x_1 at low temperature for several values of the chemical potential μ from the middle of the gap (bottom) to the band edge (top). The dashed line corresponds to the critical μ_c between dimerized and uniform phases. Inset: Enlarged view close to μ_c. The shift of μ between upper and lower bands corresponds to 7% of the Peierls gap.

This conventional Peierls scenario assumes a fixed band filling. The low-temperature insulating electronic structures found in DFT computations [8, 17, 34] correspond to half filling in the 1D model (1). However, for substrate-stabilized atomic chains, the electron chemical potential μ is determined by the substrate and may be modified by temperature and adatoms [38–40]. Therefore, we must investigate the 1D model in the grand canonical ensemble with μ set by an external electron reservoir, i.e., the rest of the In/Si(111) system. Focusing again on the decoupled 1D model, the free energies (3) are replaced by corresponding grand canonical potentials ϕ_l and ϕ.

We find that the grand canonical Peierls physics is much richer than the canonical one. Figure 4 shows the grand canonical potential of the inner chain at very low temperature as a function of the distortion amplitude for several values of μ. If μ lies at or close to the middle of the Peierls gap, we see the usual double well indicating a stable and doubly-degenerate dimerized state. When μ deviates slightly from the middle of the gap, a local minimum appears at $x = 0$ indicating that the uniform state is metastable. This case agrees qualitatively with the energetics of the phase transition in In/Si(111) calculated from first principles [18]. When μ moves even further toward the band edge, the uniform state becomes thermodynamically stable while two local minima for $x \neq 0$ show

that the dimerized states are metastable. Finally, when μ approaches the band edge, we find a single-well potential indicating that the Peierls instability is suppressed. The variation of the grand canonical potential with μ explains the sensitivity of the transition in indium wires to chemical doping [21, 38–41] and to optical excitations [18, 41]. In particular, the observation that the uniform phase is stabilized in n-doped samples [21, 41] as well as by alkali adsorption-induced charge transfer [38, 39] is naturally explained by the occurrence of a metastable uniform state in the grand canonical potential in Fig. 4.

If the temperature is raised without varying μ, the grand canonical potential changes its shape progressively into a single well but the uniform and dimerized states never exchange their relative energy positions [29]. Therefore, if we assume that μ deviates slightly from the middle of the gap, the uniform state is metastable at low temperature but the structural transition remains continuous as in the canonical ensemble. Yet the actual electronic gap closes when one of the band edges reaches μ and thus the metal-insulator transition occurs discontinuously and at a lower temperature than the structural transition.

In the 1D model, however, μ represents the influence of the substrate and thus it is a function of temperature rather than an independent parameter. (Equivalently, the dependence of the electron number on μ could change with temperature [29].) Moreover, a small change in μ is sufficient to change the shape of the grand canonical potential (see the inset of Fig. 4) and thus to cause a discontinuous transition [29]. This scenario is compatible with recent first-principles simulations and experiments [16–18, 20, 21]. Note that the dimerized configuration could be unstable toward the formation of domain walls (solitons) [37, 42, 43] but the study of spatial and thermal fluctuation effects is beyond the scope of this paper [26, 27, 30, 31, 44]. The finding of a first order transition with a small reduction of the order parameter in the critical region (see Fig. 6 in [29]) justifies the neglect of fluctuations in first approximation.

The Peierls/CDW theory predicts the existence of collective excitations (amplitude modes) which are Raman active [23, 45–47]. For the Peierls wave number Q their frequency vanishes as $\omega(T) \propto \sqrt{|T - T_c|}$ when approaching T_c in a continuous transition (phonon softening) [23, 47]. As the Peierls amplitude modes in In/Si(111) are essentially the shear and rotary modes, they should appear in the Raman spectrum at the Γ point below T_c and show significant (but incomplete) softening close to the first-order transition [29].

Figure 5 shows the temperature dependence of the normalized frequencies of some Raman spectra resonances measured for In/Si(111). The resonances observed experimentally were assigned to specific vibrational modes by comparison to first-principles computations [4, 12, 15]. Here we discuss the low-frequency modes at 20, 28, 42 cm^{-1} in the (8×2) phase and the 55 cm^{-1} mode observed for both phases, which all involve displacements

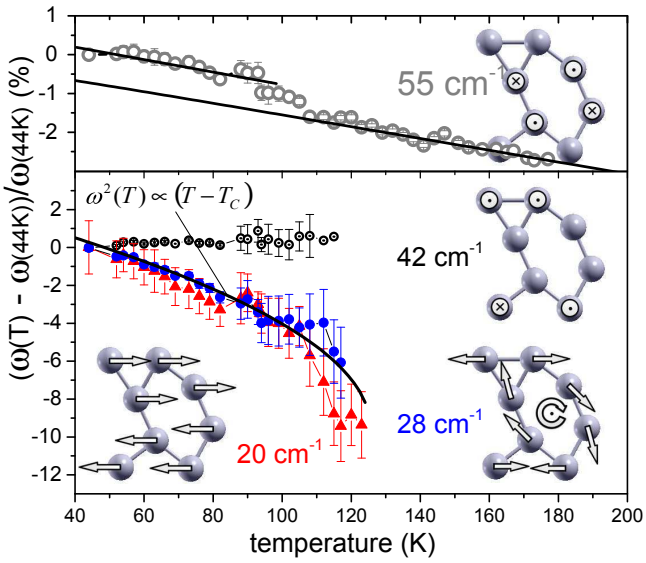

FIG. 5. (Color online) Temperature dependence of the normalized frequencies of Raman modes and sketches of the assigned eigenmodes. The shear and rotary modes (red and blue symbols) at 20 and 28 cm^{-1} are Peierls amplitude modes and exhibit a significant softening, while the mode at 42 cm^{-1} (black symbols) remains at constant frequency and the one at 55 cm^{-1} (grey symbols) shows only a moderate decrease due to the lattice expansion.

of In atoms. The resonances at 20 and 28 cm^{-1} (as measured at 44 K) are assigned to the shear and rotary modes. They exhibit a partial phonon softening when approaching the phase transition temperature and vanish above it. The mode at 42 cm^{-1}, in contrast, is at constant frequency with temperature while the mode at 55 cm^{-1} exhibits only moderate temperature shift. These observations agree qualitatively with our theoretical analysis but not with an order-disorder transition [9, 13]. The rotary and shear modes are strongly coupled to the CDW by the lateral displacements of the In atoms and show the expected softening for Peierls amplitude modes, however, this softening remains only partial because the transition is discontinuous. The 42 and 55 cm^{-1} modes, in contrast, are related to vertical displacements of In atoms. Hence they are weakly coupled to the in-plane CDW and display a behavior related to the lattice expansion with temperature increase. Remarkably, the 42 cm^{-1} mode shows no frequency shift at all, i.e. the lattice expansion is compensated by a stiffening of the involved In bonds. The 55 cm^{-1} mode displays a side-effect drop in eigenfrequency at the phase transition.

In summary, we have shown that the transition observed in In/Si(111) is a grand canonical Peierls transition. We think that the ongoing controversy about the nature of this transition can be solved by interpreting experiments and first-principles simulations [2, 3, 5–10, 13–21] within a grand canonical Peierls theory. In

particular, it explains the observation of a metastable metallic phase at low temperature and the sensitivity of the critical temperature to the substrate doping. Grand canonical theories could explain other charge-donation related phenomena in atomic wires such as the reversible structural transitions in Au/Si(553) upon electron injection [48, 49]. The present work suggests that variations of the substrate-induced chemical potential (e.g., with temperature or upon doping) is a key mechanism for understanding the realization of quasi-1D physics in atomic wires.

ACKNOWLEDGMENTS

We thank S. Wippermann for helpful discussions. This work was done as part of the Research Unit *Metallic nanowires on the atomic scale: Electronic and vibrational coupling in real world systems* (FOR1700) of the German Research Foundation (DFG) and was supported by grants Nos. JE 261/1-1. Financial support by the *Ministerium für Innovation, Wissenschaft und Forschung des Landes Nordrhein-Westfalen*, the *Senatsverwaltung für Wirtschaft, Technologie und Forschung des Landes Berlin*, and the German *Bundesministerium für Bildung und Forschung* is gratefully acknowledged.

* E-mail: eric.jeckelmann@itp.uni-hannover.de

[1] H. W. Yeom, S. Takeda, E. Rotenberg, I. Matsuda, K. Horikoshi, J. Schaefer, C. M. Lee, S. D. Kevan, T. Ohta, T. Nagao, and S. Hasegawa, Phys. Rev. Lett. **82**, 4898 (1999).
[2] P. C. Snijders and H. H. Weitering, Rev. Mod. Phys. **82**, 307 (2010).
[3] J.-H. Cho, D.-H. Oh, K. S. Kim, and L. Kleinman, Phys. Rev. B **64**, 235302 (2001).
[4] K. Fleischer, S. Chandola, N. Esser, W. Richter, and J. F. McGilp, Phys. Rev. B. **67**, 235318 (2003).
[5] T. Tanikawa, I. Matsuda, T. Kanagawa, and S. Hasegawa, Phys. Rev. Lett. **93**, 016801 (2004).
[6] J. R. Ahn, J. H. Byun, H. Koh, E. Rotenberg, S. D. Kevan, and H. W. Yeom, Phys. Rev. Lett. **93**, 106401 (2004).
[7] S.-F. Tsay, Phys. Rev. B **71**, 035207 (2005).
[8] C. González, J. Ortega, and F. Flores, New J. Phys. **7**, 100 (2005).
[9] C. González, F. Flores, and J. Ortega, Phys. Rev. Lett **96**, 136101 (2006).
[10] X. López-Lozano, A. Krivosheeva, A. A. Stekolnikov, L. Meza-Montes, C. Noguez, J. Furthmüller, and F. Bechstedt, Phys. Rev. B **73**, 035430 (2006).
[11] S. Riikonen, A. Ayuela, and D. Sańchez-Portal, Surface Science **600**, 3821 (2006).
[12] K. Fleischer, S. Chandola, N. Esser, W. Richter, and J. F. McGilp, Phys. Rev. B. **76** 205406 (2007).
[13] C. González, J. Guo, J. Ortega, F. Flores, and H. H. Weitering, Phys. Rev. Lett. **102** 115501 (2009).
[14] S. Wippermann and W. G. Schmidt, Phys. Rev. Lett. **105**, 126102 (2010).
[15] E. Speiser, S. Chandola, K. Hinrichs, M. Gensch, C. Cobet, S. Wippermann, W. G. Schmidt, F. Bechstedt, W. Richter, K. Fleischer, J. F. McGilp, and N. Esser, Phys. Status Solidi B **247**, 2033 (2010).
[16] S. Hatta, Y. Ohtsubo, T. Aruga, S. Miyamoto, H. Okuyama, H. Tajiri, and O. Sakata, Phys. Rev. B **84**, 245321 (2011).
[17] W. G. Schmidt, S. Wippermann, S. Sanna, M. Babilon, N. J. Vollmers, and U. Gerstmann, Phys. Status Solidi B **249**, 343 (2012).
[18] S. Wall, B. Krenzer, S. Wippermann, S. Sanna, F. Klasing, A. Hanisch-Blicharski, M. Kammler, W. G. Schmidt, and M. Horn-von Hoegen, Phys. Rev. Lett. **109**, 186101 (2012).
[19] H.-J. Kim and J.-H. Cho, Phys. Rev. Lett. **110**, 116801 (2013).
[20] F. Klasing, T. Frigge, B. Hafke, B. Krenzer, S. Wall, A. Hanisch-Blicharski, and M. Horn-von Hoegen, Phys. Rev. B **89**, 121107(R) (2014).
[21] H. Zhang, F. Ming, H.-J. Kim, H. Zhu, Q. Zhang, H. H. Weitering, X. Xiao, C. Zeng, J.-H. Cho, and Z. Zhang, Phys. Rev. Lett. **113**, 196802 (2014).
[22] S.-W. Kim and J.-H. Cho, Phys. Rev. B **93**, 241408 (2016).
[23] G. Grüner, *Density Waves in Solids* (Perseus Publishing, Cambridge, 2000).
[24] W.-P. Su, J. R. Schrieffer, and A. J. Heeger, Phys. Rev. Lett. **42**, 1698 (1979).
[25] W.-P. Su, J. R. Schrieffer, and A. J. Heeger, Phys. Rev. B **22**, 2099 (1980).
[26] A. J. Heeger, S. Kivelson, J. R. Schrieffer, and W.-P. Su, Rev. Mod. Phys. **60**, 781 (1988).
[27] D. Baeriswyl, D. K. Campell, and S. Mazumdar, in *Conjugated Conducting Polymers*, edited by H. Kiess (Springer, Berlin, 1992), Chap. 2.
[28] W. Barford, *Electronic and Optical Properties of Conjugated Polymers* (Oxford University Press,Oxford, 2005).
[29] See Supplemental Material at `http://dx.doi.org/10.1103/PhysRevB.93.241407` for quantitative results and additional details.
[30] E. Jeckelmann and D. Baeriswyl, Synthetic Metals **65**, 211 (1994).
[31] E. Jeckelmann, Phys. Rev. B **57**, 11838 (1998).
[32] O. Bunk, G. Falkenberg, J. H. Zeysing, L. Lottermoser, R. L. Johnson, M. Nielsen, F. Berg-Rasmussen, J. Baker, and R. Feidenhans'l, Phys. Rev. B **59**, 12228 (1999).
[33] J. Nakamura, S. Watanabe, and M. Aono, Phys. Rev. B **63**, 193307 (2001).
[34] U. Gerstmann, N. J. Vollmers, A. Lücke, M. Babilon, and W. G. Schmidt, Phys. Rev. B **89**, 165431 (2014).
[35] H. C. Longuet-Higgins and L. Salem, Proc. R. Soc. Lond. A **251**, 172 (1959).
[36] L. Salem and H. C. Longuet-Higgins, Proc. R. Soc. Lond. A **255**, 435 (1960).
[37] S. Cheon, T.-H. Kim, S.-H. Lee, and H. W. Yeom, Science **350**, 182 (2015).
[38] H. Shim, S.-Y. Yu, W. Lee, J.-Y. Koo, and G. Lee, Appl. Phys. Lett. **94**, 231901 (2009).
[39] H. Morikawa, C. C. Hwang, and H. W. Yeom, Phys. Rev. B **81**, 075401 (2010).
[40] W. G. Schmidt, M. Babilon, C. Thierfelder, S. Sanna, and

S. Wippermann, Phys. Rev. B **84**, 115416 (2011).
[41] Y. Terada, S. Yoshida, A. Okubo, K. Kanazawa, M. Xu, O. Takeuchi, and H. Shigekawa, Nano Lett. **8**, 3577 (2008).
[42] H. Zhang, J.-H. Choi, Y. Xu, X. Wang, X. Zhai, B. Wang, C. Zeng, J.-H. Cho, Z. Zhang, and J. G. Hou, Phys. Rev. Lett. **106**, 026801 (2011).
[43] T.-H. Kim and H. W. Yeom, Phys. Rev. Lett. **109**, 246802 (2012).
[44] B. Horovitz, H. Gutfreund, and M. Weger, Phys. Rev. B **12**, 3174 (1975).
[45] H. J. Schulz, Phys. Rev. B **18**, 5756 (1978).
[46] B. Horovitz, H. Gutfreund, and M. Weger, Phys. Rev. B **17**, 2796 (1978).
[47] E. Tutiš and S. Barišić, Phys. Rev. B **43**, 8431 (1991).
[48] S. Polei, P. C. Snijders, S. C. Erwin, F. J. Himpsel, K-H. Meiwes-Broer, and I. Barke, Phys. Rev. Lett. **111**, 156801 (2013).
[49] S. Polei, P. C. Snijders, K.-H. Meiwes-Broer, and I. Barke, Phys. Rev. B **89**, 205420 (2014).